Mediterranean Smart Cities Conference (MSCC 2024)
2-4 May, 2024, Martil, Morocco

RIS-aided Downlink NOMA MIMO VLC-Based IoT Devices

Mohamed El Jbari
Information and Communication Technologies Laboratory (LabTIC), National School of Applied Sciences of Tangier (ENSAT)
Abdelmalek Essaâdi University
Tangier, Morocco
mohamed.eljbari2@etu.uae.ac.ma
https://orcid.org/0000-0002-2396-9637

Mohamed Moussaoui
SIC Department, Information and Communication Technologies Laboratory (LabTIC), National School of Applied Sciences of Tangier (ENSAT)
Abdelmalek Essaâdi University
Tangier, Morocco
m.moussaoui@uae.ac.ma

***Abstract*— Internet of Things (IoT) technology has seen rapid growth, and visible light communications (VLCs) have emerged as a promising communication technology for IoT. However, challenges such as limited coverage area, blockage issues, and the need for efficient multiple-access techniques must be addressed. Additionally, the use of orthogonal time frequency space (OTFS) and reconfigurable intelligent surfaces (RISs) can potentially enhance IoT performance in low/high-mobility channels and indoor environments. Downlink VLC communication has introduced multiple-input multiple-output (MIMO) and non-orthogonal multiple access (NOMA) techniques, which have been recognized as promising for VLC-IoT systems due to their efficient resource utilization. RISs strategically configure and redirect radio signals, enhancing spectral and energy efficiency performance. This paper presents an adaptative RIS-aided VLC-IoT model based on NOMA-OTFS signals. We formulate a problem maximizing the channel capacity with an optimal solution using an algorithm with low complexity. Our results demonstrate that NOMA-based OTFS modulation has been observed to outperform OFDM in mobility channels, with a high RIS-assisted MIMO VLC-IoT system capacity.**

Keywords—IoT; VLC; RIS; MIMO; NOMA-OTFS; adaptative capacity.

I. INTRODUCTION

Internet of Things (IoT) technology has rapidly expanded over the last decade, with a 16.9 percent compound annual growth rate, reaching $1.7 trillion and approximately 27 billion devices connected to the Internet at the beginning of the 2020s [1]. Visible light communications (VLCs) have emerged as a promising IoT communication technology, which provides many attractive features that the radiofrequency (RF)-based IoT networks [2]. In addition, it offers features such as accurate device positioning, energy harvesting from light, and inherent physical-layer (PHY) security [3,4]. VLC-IoT aims to create a bidirectional wireless communication system using visible light in the downlink, leveraging existing light emitting diode (LED) fixtures for both communication and illumination purposes in the uncultivated spectrum i., e. $400nm - 800nm$ [5], [6].

VLC can provide high-speed data transfer by using transceivers with minimal energy consumption, and exceptionally dense networking, and existing RF communications have little interference benefit [7]. However, according to a market assessment, around 96% of IoT data is produced inside, and this is in line with the needs of VLC-based IoT applications [8].

Lately, much research has been done on this topic, such as on simultaneous Lightwave information and power transmission [9], VLC backscattering-enabled self-charging IoT devices, VLC-IoT physical layer security [4], etc. However, many difficulties need to be solved before VLC-IoT becomes widely used. First, the high-path loss of the lightwave limits the coverage area of a VLC transmitter [10], which affects the communication between the controller system and the optical IoT devices [1]. Secondly, the blockage issue can severely impair the performance of VLC-IoT given the lightwave's infinite absorption loss. Multiple IoT devices should be supported by the VLC access point (AP) of an optical photodiode (PD) in VLC-IoT networks, as ubiquitous IoT is often needed to connect many IoT devices per unit of space [4]. Thus, to properly apply VLC-IoT in real-world applications, an effective multiple-access approach is crucial. For visible light-based downlink VLC communication, several multiple access approaches have been presented at this point. These techniques fall into two main techniques: orthogonal multiple access (OMA) and non-orthogonal multiple access (NOMA) [11]. Through successive interference cancellation (SIC) and power domain superposition coding (SPC), NOMA enables many users to concurrently exploit all time and frequency resources [12]. Because of its

efficient allocation of resources, NOMA has been recognized as a viable multiple-access solution for multi-user VLC systems [15]–[20]. Users are allotted distinct orthogonal time or frequency resources for OMA methods such as time division multiple access (TDMA) and orthogonal frequency division multiple access (OFDMA) [11]–[13]. High spectral efficiency (SE) and resistance to inter-symbol interference (ISI) caused by dispersive wireless channels led to the selection of OFDM [6], [7]. Multiple users and multiple transmitter antenna situations were shown to benefit from OFDM [8], [9]. However, in the context of the more complex network required for next-generation (6G) wireless systems, where Doppler shifts of various users are high or cannot be reliably predicted, OFDM faces challenges from time-frequency carrier offsets and also out-of-band (OOB) emissions [10]. Consequently, the Doppler shift of the channel reduces the orthogonality that exists between subcarrier frequencies, leading to a rise in inter-carrier interference (ICI) inside the network [11], [12]. Many attempts have been made in the scientific literature [13], [16], and [17] to reduce the ICI-related issues caused by a doubly selective channel.

Orthogonal time frequency space (OTFS) [13], [18] was proposed considering this introduction. The cutting-edge modulation format known as OTFS modifies the standard process for mapping information symbols. Traditional mapping places the symbols in the time or frequency domain as OFDM, but OTFS maps the symbols to the delay-Doppler (DD) domain. OTFS is an innovative two-dimensional (2D) modulation technique that enables orthogonality and separability between carrier waveforms for the doubly selective channel, enabling very dispersive gain [19]. Both static multipath channels and high-mobility channels can benefit from OTFS's enhanced performance. In [19], [9], the effectiveness of OFDM and OTFS for low mobility channels was examined, with OTFS performing better.

To guarantee widespread high-speed connectivity, we still have a few obstacles to overcome. First and foremost, we need to provide perfect interior network coverage. Random natural and artificial obstacles such as walls, obstacles, objects, etc., hinder the non-line of sight (NLoS) path in indoor VLC communications, in addition to the line of sight (LoS). Multipath interference results from uncontrolled transmitted signals interacting with random objects in the surrounding environment, lowering the quality of the received signals [7]. High Doppler shifts, severe attenuation, ISI, and deep fading are the key propagation problems [9]. Although numerous PHY solutions, including adaptive single-multicarrier modulations, coding [7–10], cooperative communications, and multiple-input multiple-output (MIMO), have been developed, PHY technology has not advanced enough to satisfy the required reliability and maximum bandwidth capacity channel. Furthermore, the adopted technologies fail to guarantee the network's quality of service (QoS) due to the variable nature of the propagation medium. The concept of using a reconfigurable intelligent surface (RIS) as a remedy has garnered a lot of attention lately. RISs may strategically adjust and divert the radio signal impinged upon them when positioned between the transmitter and the receiver. The specifics of RIS's construction and design are covered in [15]. A flawlessly conducting sheet examined on its own provides insight into the optimal functioning of RIS. This passive surface spreads the incoming signal at an angle determined by the generalized Snell's law of reflection, serving as a reflecting mirror for the incoming RF waves. The improvement of RIS-assisted systems' performance in energy efficiency (EE), SE, and other areas has been extensively researched [15,20].

We investigated NOMA-OTFS modulation for the suggested RIS-assisted VLC-IoT in this research. To the best of our knowledge, no research has been done on OTFS-based downlink NOMA for the RIS-VLC-IoT system. Then, the following may be used to describe our contribution to this study:

1) For the 2D VLC-IoT system, an EE downlink NOMA method based on OTFS modulation is used. The system uses a QoS-guaranteed optimum power allocation resource (PAR) technique to optimize the EE.

2) We characterize the channel modeling of proposed RIS-enabled NOMA-OTFS in two domains DD and TF for VLC-IoT. The performance of our system has been obtained using maximum likelihood (ML) as a detector, and compared with the OFDM.

3) Based on the peak power intensity transmitted by LED, When both the counterpart upper bound and the capacity lower bound converge to the same expression, the maximum capacity expressions in the high-signal-to-noise ratio (SNR) scenario may be produced. Concerning the alignment of the RIS elements and the PAR vectors, the capacity maximization problem is expressed.

4) We present the solution optimization approach, which has low complexity owing to the upper-bound solution to this issue, to increase the capacity of the RIS-aided NOMA-OTFS VLC-IoT system. Lastly, the numerical results surpass the effectiveness of the suggested method and demonstrate the capacity maximization of the RIS-aided downlink of the NOMA-OTFS VLC system with their QoS-IoT using a relaxing algorithm.

The results show that NOMA's adoption of PAR with adaptive channel and QoS-based user for an EE of VLC-IoT systems is superior.

This is how the rest of the paper is structured. The system concept, the VLC-IoT principle, downlink NOMA-OTFS processing, and its use for SE and EE of RIS-assisted VLC-IoT communication are all addressed in Section II. In Section III, the issue formulation is presented together with an ideal solution. In Section IV, the comprehensive simulation results are examined and discussed. Section VI provides a short conclusion of this paper's findings.

Notations: In this article, scalers are indicated by regular letters like x or X, while vectors/matrices are denoted by boldface letters like $\boldsymbol{x}$ or $\boldsymbol{X}$. The matrix transpose, vectorization operator, and block diagonal matrix are thus denoted by $(\cdot)^T$, $vec(\cdot)$, and $Diag(.)$. The n-th main diagonal vector is supplied by x_n, and the off-diagonal elements are zeros, respectively. Note that $f(\boldsymbol{G}; P_u)$ denotes a function concerning a with the fixed P_u.

Let $\boldsymbol{F_N}\otimes\boldsymbol{I_M}$ the convolution product between the $M \times M$ identity matrix $\boldsymbol{I_M}$ and N-point discrete Fourier transform (DFT) matrix $\boldsymbol{F_N}$ with an N-point inverse DFT (IDFT) matrix $\boldsymbol{F_N^H}$.The $\mathbb{C}^+$denotes complex number set with real values.

II. SYSTEM MODEL

In this section, we presented the basic model of the VLC-IoT system, which can configure the VLC-IoT system with a bidirectional light model based on both paths, i., e. LoS and the NLoS. Then, the downlink NOMA VLC-IoT with OTFS modulation is presented with a noise model at the transmitter. The system model of RIS-enabled VLC-IoT is given based on the law of Snell's and indirect NLoS link. At the receiver end, a detection and demodulation process is applied to recover the data information for IoT devices.

A. Two-dimensional VLC-IoT System

This research examines a 2D VLC-IoT system, as seen in Figs. 1 and 2. The OMA downlink uses the wave light from the LED for synchronous lighting and communication, while the RIS element uses reflected light for NOMA communication.

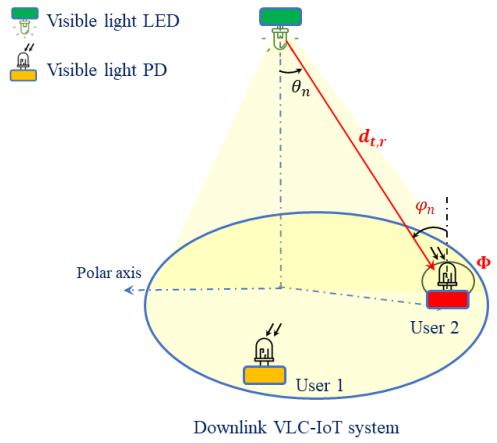

Figure. 1. NOMA downlink VLC-IoT system.

Let n_t-th $\in \{1, \dots, N_t\}$ LED and n_s-th $\in \{1, \dots, N_{RIS}\}$RIS reflected elements. The VLC system's channel gain is dependent on the transceiver positions; consequently, the considered RIS-assisted MIMO VLC channel is narrowband and time-invariant within the coherent time. This can be represented by a vector $\boldsymbol{h} \triangleq [h_1, \dots, h_{N_t}]^T \in \mathbb{C}^+_{N_t N_r}$, where h_n signifies the superimposed channel gain between the n_t-th LED and the n_r-th PD; nonetheless, the RIS-assisted MIMO-VLC's channel gain is made up of the direct LoS channel $\boldsymbol{h_n^{LoS}}$ and the indirect NLoS channel of the reflected RISs $\boldsymbol{h_n^{NLoS}}$, which are modeled as follows

$$\boldsymbol{h} = \boldsymbol{h_n^{LoS}} + \boldsymbol{h_n^{NLoS}}. \quad (1)$$

Intensity modulation/direct detection (IM/DD) scheme is applied in indoor VLC application[8], all entries of $\boldsymbol{h_n^{LoS}}$ and $\boldsymbol{h_n^{NLoS}}$are the positive real-valued. For the visible light LED with a Lambertian emission pattern, the direct current (DC) has a LoS channel gain between the LED and the u-th $(u = 1, 2, \dots, U)$ user for the NOMA downlink channel can expressed as [7]

$$h_n^{LoS} = \begin{cases} \frac{\mathcal{R}_p \mathcal{A}_p (m+1)}{2\pi d_{t,n}^2 \sin^2 \varphi_n} \rho_r \mathcal{T}_{OF} \cos^m \theta_n \cos \varphi_n, & 0 \le \varphi_n \le \Phi \\ 0, & \varphi_n > \varphi_n \end{cases}, \quad (2)$$

where $\mathcal{R}_p$, $\mathcal{A}_p$, ρ_r, $\mathcal{T}_{OF}$ represent the photoresponsivity and area of PD, the refractive index of RISs and optical filter gain, respectively. Let $m = -ln2/\ln(cos\ \phi_{1/2})$ is the Lambertian order with $\phi_{1/2}$ the semi-angle of light LED. θ_n, φ_n , and Φ are the corresponding emission angle, the incident angle at RISs, and the field-of-view (FOV) angle of the PD.

In indirect NLoS, we propose an alignment binary matrix $\boldsymbol{G} \triangleq [g_1, \dots, g_{N_t}] \in \{0,1\}^{N_t N_{RIS}}$between the LEDs and RIS-element, which started from n_t -th LED to reflected n_s-th RISs and finally received by n_r-th PDs. As results, the NLoS channel gain is expressed as

$$h_n^{LoS} = \frac{\mathcal{R}_p \mathcal{A}_p (m+1)}{2\pi (d_{t,n} + d_{n,r})^2 \sin^2 \varphi_{n,r}} \rho_r \mathcal{T}_{OF} \cos^m \theta_{n,r} \cos \varphi_{n,r}, (3)$$

where $\theta_{n,r}$ and $\varphi_{n,r}$ denote the angle of brightness at the LED and the angle of incidence at the PD, respectively. $d_{t,n}$, and $d_{n,r}$ represent the distance from the n_t-th LED to the n_s -th RIS, and the distance from the n_s -th RISs reflecting elements to the n_r-th PD, respectively. So, the NLoS channel gain of RISs can be written as follows

$$\boldsymbol{h_n^{LoS}} = dig(\boldsymbol{H})^T vec(\boldsymbol{G}), \quad (4)$$

where $\boldsymbol{H} \triangleq [\boldsymbol{h}_{1,1}, \dots, \boldsymbol{h}_{N_t N_r}] \in \mathbb{C}^+_{N_t N_r}$ denotes the matrix channel from n_t-th LED to n_r-th PD.

B. NOMA-OTFS for Downlink VLC-IoT

This section assumes that the VLC-IoT system serves U = 2 users and uses the downlink NOMA, which is not the loss. The schematic diagram of the VLC-IoT downlink with NOMA enabled is shown in Fig. 3. The modulated data signals meant for the far away and near users, respectively, are indicated by the symbols s_{u1} and s_{u2}. The power domain superposition is carried out for the two users inside each user. Therefore, the u-th user's superposed electrical signal may be described as

$$x_u = \sqrt{p_{u1}} s_{u1} + \sqrt{p_{u2}} s_{u2}, \quad (5)$$

where p_{u1} and p_{u2} are the NOMA downlink electrical transmit powers allocated to the far and near users, respectively. The DCO-OTFS current I_{DC} is added to the

resulting signal after power domain superposition, inter-pair bandwidth allocation, and a DC optical bias current modulated by OTFS modulation, as shown in (6), to simultaneously ensure the positif driving signal of the visible light LED in the VLC and guarantee sufficient and stable illumination. The total downlink NOMA electrical transmit power is distributed across all users as $P_e = p_{u1} + p_{u2}$.

The source bits are first translated to a set of 4-QAM symbols in OTFS modulation, and the resultant QAM symbols are subsequently transformed into a two-dimensional DD grid [9], as opposed to using the 2D time-frequency (TF) grids. We take into consideration the OTFS transmit frames, which are composed of *(M ×N)* 4-QAM symbols mapped to DD symbols $\boldsymbol{S}_u \in \mathbb{C}^{M\times N}$. The inverse symplectic Fourier transform (ISFFT) is used in a two-step conversion process to convert the DD symbols into TD signals as follows

$$\boldsymbol{X}_u = \boldsymbol{S}_u \boldsymbol{F}_M^H, \quad (6)$$

The transmit TD matrix is vectorized to the TD $\boldsymbol{x}_u \in \mathbb{C}^{MN\times 1}$ vectors as

$$\boldsymbol{x}_u = \mathrm{vec}(\boldsymbol{X}_u) = (\boldsymbol{F}_M^H \otimes \boldsymbol{I}_M)\boldsymbol{s}_u, \quad (7)$$

After that, the single cyclic prefix (CP) of frame length is added to reduce ISI and raise SE.

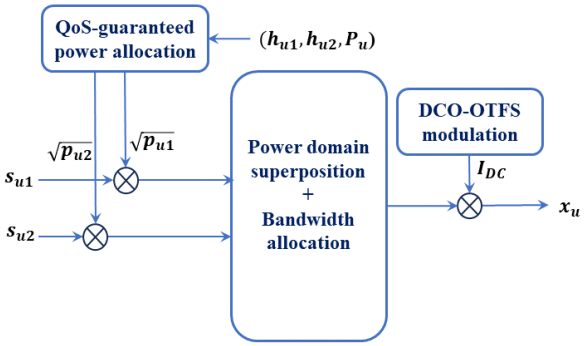

Figure 2. Schematic diagram of downlink NOMA-enabled VLC-IoT.

C. RIS-assisted VLC-IoT

The signal that the RIS receives travels across a regulated propagation medium. Every RIS processing component will have a phase shift that corresponds to the OTFS modulated signal that is incident upon it. One may write the TD signal that was received at the n_s-th RIS element as

$$r_u = \iint h_n(\tau,\nu)\, x_u(t-\tau) e^{-j2\pi\nu(t-\tau)} d\tau d\nu + \omega_{t,n}, \quad (8)$$

Then,

$$\boldsymbol{r}_u = \sqrt{P_e}\mathbf{H}\boldsymbol{x}_u + \boldsymbol{w}_u, \quad (9)$$

where $h = h_{\tau,\nu}$ denotes the channel impulsion response with a delay τ and Doppler ν in TF grids with the corresponding AWGN term $\omega_{t,n}$ [9]. The phase shift by which the signal is reflected towards the receiver is taken into consideration for channel SNR maximization. This may be calculated from (9) and is given by

$$SNR = \frac{P_e|H|^2}{\boldsymbol{w}}, \quad (10)$$

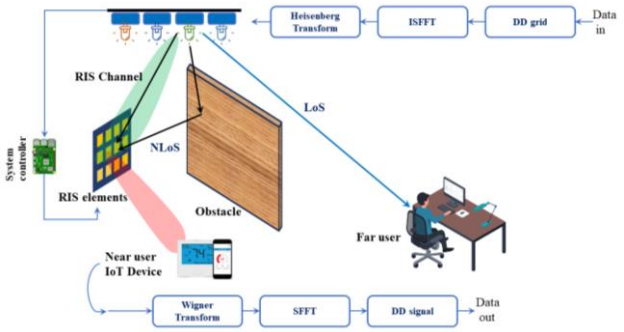

Figure. 3 RIS-aided NOMA-OTFS modulation for MIMO VLC-IoT system.

D. Detection and receiver processing

The TD signal $\boldsymbol{r}_u$ was received at the PD end is first de-vectorized to the $M \times N$ TF matrix $\boldsymbol{R}_u$, and converted it into the DD domain using OTFS demodulation by applying the SFFT, and then the DD signal is detected using an ML detector.

$$\boldsymbol{y}_u = \mathrm{vec}(\boldsymbol{Y}_u) = (\boldsymbol{F}_N \otimes \boldsymbol{I}_M)\boldsymbol{r}_u, \quad (11)$$

The received downlink signals of the nearby and far users in the u-th user may be obtained by deleting the DC term, which are given as

$$y_{u1} = \boldsymbol{h}_{u1}^T \boldsymbol{x}_{u,n} + z_{u1}, \quad (12)$$

$$y_{u2} = \boldsymbol{h}_{u2}^T \boldsymbol{x}_{u,n} + z_{u2}, \quad (13)$$

where $\boldsymbol{x}_{u,n} \triangleq [\boldsymbol{x}_{u,1}, \boldsymbol{x}_{u,2}, \ldots, \boldsymbol{x}_{u,N_t}]^T \in \mathbb{C}_{N_t N_r}^+$ denotes the light signal transmitted by n_t-LED and received by n_r-PD. $\boldsymbol{h}_{u,1}$, and $\boldsymbol{h}_{u,2}$ are the channel gain of the far and near users, respectively, and z_{u1}, z_{u1} are the corresponding zero-mean of additive white Gaussian noises (AWGN) with the variance of σ^2 and $\boldsymbol{h}_{u,1} \leq \boldsymbol{h}_{u,2}$.

III. PROBLEM FORMULATION AND OPTIMISATION

In this part, we use various theoretical techniques to determine the channel capacity provided to us. To be more precise, $Q(\boldsymbol{x_u})$, $R(\boldsymbol{y_u})$, and $W(\boldsymbol{y_u}|\boldsymbol{x_u})$, stand for the probability measure of input $\boldsymbol{x_u}$, output $\boldsymbol{y_u}$, and the transition probability, respectively. Then, the their mutual information is defined as $I(\boldsymbol{x_u}; \boldsymbol{y_u})$, and the Kullback–

Leibler (KL) divergence $D(\boldsymbol{x_u}||\boldsymbol{y_u})$. Let "sup" is the supremum of the function, where, the capacity of the RIS-aided NOMA downlink MIMO VLC can be reformulated as [20]

$$\mathcal{C}(P_u, P_e) = \sup_{Q(\boldsymbol{x_u})} I(Q(\boldsymbol{x_u}); W(\boldsymbol{y_u}|\boldsymbol{x_u})), \tag{13}$$

The asymptotic capacity channel in the high-SNR regime of the NOMA downlink MIMO VLC-IoT is given as

$$\mathcal{C}(P_u, P_e) = \begin{cases} \mathcal{C}(\boldsymbol{G}, P_u) = \frac{1}{2} log\left(\frac{\left(\boldsymbol{h}_{n,u}^T P_u\right)^2}{2\pi e\sigma^2}\right), \ P_u \to \infty \\ \mathcal{C}(\boldsymbol{G}, P_e) = \frac{1}{2} log\left(\frac{e\left(\boldsymbol{h}_{n,u}^T P_e\right)^2}{2\pi\sigma^2}\right), \ P_e \to \infty \end{cases}, \tag{14}$$

As results, we expressed a generalized capacity maximization problem of the proposed RIS-assisted MIMO VLC-IoT system, Hence, the objective function is formulated as

$$f(\boldsymbol{G}, P_u) \triangleq \log\left(\boldsymbol{h}_{n,u}^T P_u\right), \tag{15}$$

For the rest of the step of optimal solution this problem, we propose an algorithm as shown in Algorithm 1.

Algorithm 1 Maximum capacity and QoS-based IoT device

Input: $h_{n,u}$, $\mathcal{C}_u$, P_u, $u = 1,2$
Output: *optimal channel capacity* $\mathcal{C}_u$ *of U users.*
Step 1: channel-based user
Update channel gain $(h_{n,u})_{u=1,2}$ *in ascending order*
Inti G: $g_{n,u} = 1$, *if* $u1 = \arg\min_{u2} d_{n,u2}$
$g_{n,u} = 0$, *if* $u1 = u2$
Inti $\boldsymbol{P_e}$***:*** $P_u = \min(P_e/N_t, P_{u,max})$
repeat
Set $n \to 1$
repeat
Calculate $P_{u,min}$ *using* $\mathcal{C}_u$
Step 2: QoS-based IoT device
Sort maximum $\mathcal{C}_u$
Obtain $\mathcal{C}_u = \{(G_u, P_u); (G_u, P_e)\}$ *using (14) and (15)*
for $u = 1$ *to 2* ***do***
if $P_u \le P_e \le 0$ ***then***
Break
else
$\mathcal{C}_{u1} = \mathcal{C}_{u2}$
end if
Update LED index $n \to n + 1$
end for

I. NUMERICAL RESULTS

In this section, we consider the MIMO downlink of an RIS-assisted VLC-IoT system indoor room dimension, where both n-th LED and RIS have been equipped with regular planar arrays. Table I presents all simulation used to obtain the following results concerning the capacity maximization and QoS-based VLC-IoT system, not forgetting the BER performance on our paper. Fig. 4 shows the SNR performance comparison at IoT devices locations in an indoor room dimension. . It is observed that near IoT device to RIS element position achieves a remarkable SNR over than the other devices.

TABLE I. SIMULATION PARAMETERS

Parameter	Value
Lambertien index, m	1
Room dimension	$(5\ m, 5\ m, 3.5\ m)$
Reflectivity, ρ_r	0.9
Photoresponsivity of PD, $\mathcal{R}_p$	$0.4\ A/W$
Bandwidth system	50 MHz
Semi-angle of FoV,	70°
Maximum peak power on LEDs, $P_{u,max}$	$1.5\ W$
Optical filter gain, $\mathcal{T}_{OF}$	1
Maximum vertical distance LED-PD, $d_{n,r}$	$2.85\ m$
Number of RIS, N_{RIS}	12
Number of LED, N_t	4
Number of PD, N_r	2
SNR	$10 - 45\ dB$

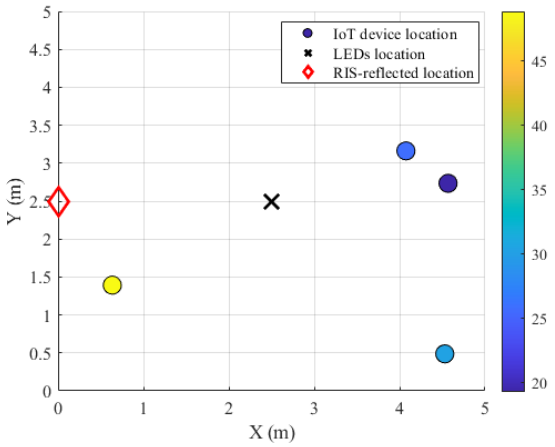

Figure 4. the high SNR at IoT device locations.

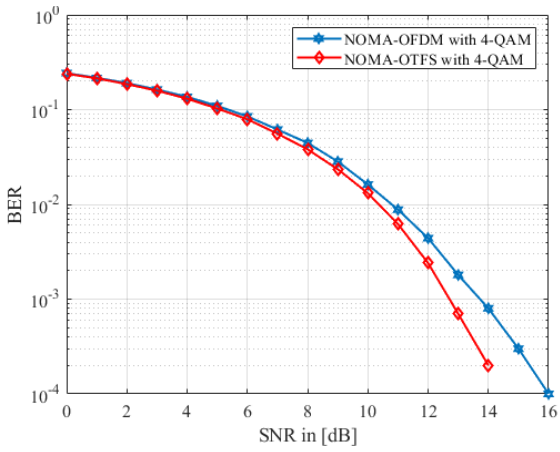

Figure 5. the BER as function a SNR value of both models.

Fig. 5 illustrates the performance metric of BER for proposed NOMA-OTFS modulation scheme and

benchmarks scheme with some modulation order 4-QAM. As shown in Fig. 5, NOMA-OTFS can gain to 2 dB compared to traditional NOMA-based OFDM at BER value of 10^{-4} . In addition, NOMA-based OTFS modulation achieve a low peak average power ratio than OFDMA scheme.

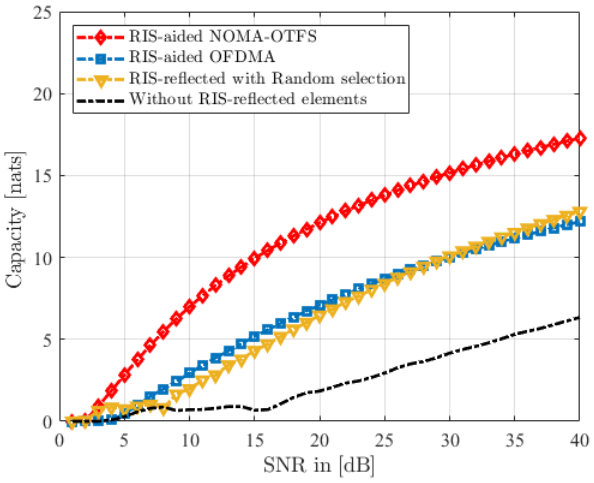

Figure 6. Capacity optimization of MIMO VLC-IoT system.

The adaptative capacity of MIMO VLC-IoT system versus SNR values is showed in Fig. 6. From these results we can observe the performance of our model with maximum capacity superior to the benchmark schemes. The capacity obtained by RIS-aided MIMO VLC-IoT based on NOMA-OTFS modulation achieves a 17.5 $nats$, that can confirm the importance of our algorithm to maximize it's with a low complexity of $\mathcal{O}(N_t N_{RIS} N_r)$.

II. CONCLUSION AND PERSPECTIVE

In this paper, we establish a RIS-enhanced MIMO VLC-based IoT system with channel modeling using a novel NOMA-OTFS modulation. The channel capacity maximization is the object of this work with a resolution problem of its. We derived an expression of channel capacity dependent of power allocation of each user and the total power emitted by the LEDs in high SNR conditions. As results a, the numerical simulation was shown the performance of our model for indoor VLC-IoT with low BER.

ACKNOWLEDGMENT

A work-in-progress is being presented for potential publication at the Mediterranean Smart Cities Conference (MSCC 2024). By turning in this work, we particularly thank Mr. Mohamed Moussaoui for his tireless efforts in bringing this research project to fruition, as well as the MSCC organizers.

REFERENCES

[1] Muhammad Sarmad Mir, Borja Genoves Guzman, Ander Galisteo, and Domenico Giustiniano. 2020. Non-linearity of LEDs for VLC IoT applications. In Proceedings of the Workshop on Light Up the IoT (LIOT '20). Association for Computing Machinery, New York, NY, USA, 6–11.

[2] Y. Mehmood, F. Ahmad, I. Yaqoob, A. Adnane, M. Imran, and S. Guizani, "Internet-of-Things-based smart cities: Recent advances and challenges," *IEEE Commun. Mag.*, vol. 55, no. 9, pp. 16–24, Sep. 2017.

[3] I. Bouziane, H. Belmokadem and M. Moussaoui, "A Review of Formal Security Verification of Common Internet of Things (IoT) Communication Protocols," 2023 7th IEEE Congress on Information Science and Technology (CiSt), Agadir - Essaouira, Morocco, 2023, pp. 334-341.

[4] A. Sharma and H. Bhatt, "Increasing Physical Layer Security Through Hyperchaos in VLC Systems," SN Computer Science, vol. 4, no. 2, p. 155, 2023.

[5] El Jbari, M., Moussaoui, M., & Chahboun, N. (2021, November). A review on visible light communication system for 5G. In International Conference on Advanced Technologies for Humanity (pp. 84-95). Cham: Springer International Publishing.

[6] El Jbari, M., & Moussaoui, M. (2022). Efficient nM-PAWM hybrid modulation scheme for high data transmission in visible light communication system. e-Prime-Advances in Electrical Engineering, Electronics and Energy, 2, 100061.

[7] El Jbari, M., & Moussaoui, M. (2023). The hybrid pulse amplitude width modulation scheme: high efficiency technique for dimmable VLC systems. Journal of Optical Communications, (0).

[8] H. Yang, W.-D. Zhong, C. Chen, A. Alphones, and P. Du, "QoS-driven optimized design-based integrated visible light communication and positioning for indoor IoT networks," IEEE Internet Things J., vol. 7, no. 1, pp. 269–283, Jan. 2020

[9] El Jbari, M., & Moussaoui, M. (2024). Efficient downlink MU-MIMO VLC systems with NOMA-OTFS modulation for indoor applications. Optical Engineering, 63(2), 028102-028102.

[10] M. El Jbari and M. Moussaoui, "Energy Efficient Channel Coding for Terahertz Communications in 6G Networks," 2022 International Conference on Innovation and Intelligence for Informatics, Computing, and Technologies (3ICT), Sakheer, Bahrain, 2022, pp. 481-488, doi: 10.1109/3ICT56508.2022.9990857.

[11] Z. Ding, X. Lei, G. K. Karagiannidis, R. Schober, J. Yuan, and V. K. Bhargava, "A survey on non-orthogonal multiple access for 5G networks: Research challenges and future trends," IEEE J. Sel. Areas Commun., vol. 35, no. 10, pp. 2181–2195, Oct. 2017.

[12] T. Dean, M. Chowdhury, and A. Goldsmith, ''A new modulation technique for Doppler compensation in frequency-dispersive channels,'' in *Proc. IEEE 28th Annu. Int. Symp. Pers., Indoor, Mobile Radio Commun. (PIMRC)*, Oct. 2017, pp. 1–7.

[13] B. Farhang-Boroujeny, ''Filter bank spectrum sensing for cognitive radios,'' *IEEE Trans. Signal Process.*, vol. 56, no. 5, pp. 1801–1811, May 2008.

[14] V. Vakilian, T. Wild, F. Schaich, S. ten Brink, and J.-F. Frigon, ''Universalfiltered multi-carrier technique for wireless systems beyond LTE,'' in *Proc. IEEE Globecom Workshops (GC Wkshps)*, Dec. 2013, pp. 223–228.

[15] Q.-U.-A. Nadeem, A. Kammoun, A. Chaaban, M. Debbah, and M.-S. Alouini, "Asymptotic max-min SINR analysis of reconfigurable intelligent surface assisted MISO systems," *IEEE Trans. Wireless Commun.*, vol. 19, no. 12, pp. 7748–7764, Dec. 2020

[16] G. Fettweis, M. Krondorf, and S. Bittner, ''GFDM–Generalized frequency division multiplexing,'' in *Proc. VTC Spring - IEEE 69th Veh. Technol. Conf.*, Apr. 2009, pp. 1–4.

[17] R. Hadani, S. Rakib, M. Tsatsanis, A. Monk, A. J. Goldsmith, A. F. Molisch, and R. Calderbank, ''Orthogonal time frequency space modulation,'' in *Proc. IEEE Wireless Commun. Netw. Conf. (WCNC)*, Mar. 2017, pp. 1–6..

[18] P. Raviteja, K. T. Phan, Y. Hong, and E. Viterbo, ''Interference cancellation and iterative detection for orthogonal time frequency space modulation,'' *IEEE Trans. Wireless Commun.*, vol. 17, no. 10, pp. 6501–6515, Oct. 2018.

[19] G. D. Surabhi and A. Chockalingam, ''Low-complexity linear equalization for OTFS modulation,'' *IEEE Commun. Lett.*, vol. 24, no. 2, pp. 330–334, Feb. 2020.

[20] W. Tang et al., "MIMO transmission through reconfigurable intelligent surface: System design, analysis, and implementation," *IEEE J. Sel. Areas Commun.*, vol. 38, no. 11, pp. 2683–2699, Nov. 2020.